Measurement of Λ_b production and lifetime in Z^0 hadronic decays

DELPHI Collaboration

P. Abreu[t], W. Adam[g], T. Adye[ak], E. Agasi[ad], I. Ajinenko[aq], R. Aleksan[am], G.D. Alekseev[n],
A. Algeri[m], P. Allen[aw], S. Almehed[w], S.J. Alvsvaag[d], U. Amaldi[g], A. Andreazza[aa], P. Antilogus[x],
W-D. Apel[o], R.J. Apsimon[ak], Y. Arnoud[am], B. Asman[as], J-E. Augustin[r], A. Augustinus[ad],
P. Baillon[g], P. Bambade[r], F. Barao[t], R. Barate[ℓ], G. Barbiellini[au], D.Y. Bardin[n], G.J. Barker[ah],
A. Baroncelli[ao], O. Barring[g], J.A. Barrio[y], W. Bartl[ay], M.J. Bates[ak], M. Battaglia[m],
M. Baubillier[v], K-H. Becks[ba], C.J. Beeston[ah], M. Begalli[aj], P. Beilliere[f], Yu. Belokopytov[aq],
P. Beltran[i], D. Benedic[h], A.C. Benvenuti[e], M. Berggren[r], D. Bertrand[b], F. Bianchi[at],
M.S. Bilenky[n], P. Billoir[v], J. Bjarne[w], D. Bloch[h], S. Blyth[ah], V. Bocci[aℓ], P.N. Bogolubov[n],
T. Bolognese[am], M. Bonesini[aa], W. Bonivento[aa], P.S.L. Booth[u], G. Borisov[aq], H. Borner[g],
C. Bosio[ao], B. Bostjancic[ar], S. Bosworth[ah], O. Botner[av], B. Bouquet[r], C. Bourdarios[r],
T.J.V. Bowcock[u], M. Bozzo[k], S. Braibant[b], P. Branchini[ao], K.D. Brand[ai], R.A. Brenner[g],
H. Briand[v], C. Bricman[b], R.C.A. Brown[g], N. Brummer[ad], J-M. Brunet[f], L. Bugge[af], T. Buran[af],
H. Burmeister[g], J.A.M.A. Buytaert[g], M. Caccia[g], M. Calvi[aa], A.J. Camacho Rozas[ap],
R. Campion[u], T. Camporesi[g], V. Canale[aℓ], F. Cao[b], F. Carena[g], L. Carroll[u], C. Caso[k],
M.V. Castillo Gimenez[aw], A. Cattai[g], F.R. Cavallo[e], L. Cerrito[aℓ], V. Chabaud[g], A. Chan[a],
M. Chapkin[aq], Ph. Charpentier[g], L. Chaussard[r], J. Chauveau[v], P. Checchia[ai], G.A. Chelkov[n],
L. Chevalier[am], P. Chliapnikov[aq], V. Chorowicz[v], J.T.M. Chrin[aw], P. Collins[ah],
J.L. Contreras[y], R. Contri[k], E. Cortina[aw], G. Cosme[r], F. Couchot[r], H.B. Crawley[a],
D. Crennell[ak], G. Crosetti[k], M. Crozon[f], J. Cuevas Maestro[ag], S. Czellar[m], E. Dahl-Jensen[ab],
B. Dalmagne[r], M. Dam[af], G. Damgaard[ab], E. Daubie[b], A. Daum[o], P.D. Dauncey[ah],
M. Davenport[g], P. David[v], J. Davies[u], W. Da Silva[v], C. Defoix[f], P. Delpierre[f], N. Demaria[at],
A. De Angelis[au], H. De Boeck[b], W. De Boer[o], C. De Clercq[b], M.D.M. De Fez Laso[aw],
N. De Groot[ad], C. De La Vaissiere[v], B. De Lotto[au], A. De Min[aa], H. Dijkstra[g], L. Di Ciaccio[aℓ],
J. Dolbeau[f], M. Donszelmann[g], K. Doroba[az], M. Dracos[g], J. Drees[ba], M. Dris[ae], Y. Dufour[g],
F. Dupont[ℓ], D. Edsall[a], L-O. Eek[av], P.A.-M. Eerola[g], R. Ehret[o], T. Ekelof[av], G. Ekspong[as],
A. Elliot Peisert[ai], J-P. Engel[h], N. Ershaidat[v], D. Fassouliotis[ae], M. Feindt[g], A. Fenyuk[aq],
M. Fernandez Alonso[ap], A. Ferrer[aw], T.A. Filippas[ae], A. Firestone[a], H. Foeth[g], E. Fokitis[ae],
F. Fontanelli[k], K.A.J. Forbes[u], J-L. Fousset[z], S. Francon[x], B. Franek[ak], P. Frenkiel[f],
D.C. Fries[o], A.G. Frodesen[d], R. Fruhwirth[ay], F. Fulda-Quenzer[r], K. Furnival[u], H. Furstenau[o],
J. Fuster[g], D. Gamba[at], C. Garcia[aw], J. Garcia[ap], C. Gaspar[g], U. Gasparini[ai], Ph. Gavillet[g],
E.N. Gazis[ae], J-P. Gerber[h], P. Giacomelli[g], R. Gokieli[az], B. Golob[ar], V.M. Golovatyuk[n],
J.J. Gomez Y Cadenas[g], G. Gopal[ak], L. Gorn[a], M. Gorski[az], V. Gracco[k], A. Grant[g],
F. Grard[b], E. Graziani[ao], G. Grosdidier[r], E. Gross[g], P. Grosse-Wiesmann[g], B. Grossetete[v],
J. Guy[ak], U. Haedinger[o], F. Hahn[ba], M. Hahn[o], S. Haider[ad], Z. Hajduk[p], A. Hakansson[w],
A. Hallgren[av], K. Hamacher[ba], G. Hamel De Monchenault[am], W. Hao[ad], F.J. Harris[ah],
V. Hedberg[w], T. Henkes[g], J.J. Hernandez[aw], P. Herquet[b], H. Herr[g], T.L. Hessing[u],
I. Hietanen[m], C.O. Higgins[u], E. Higon[aw], H.J. Hilke[g], S.D. Hodgson[ah], T. Hofmokl[az],
S-O. Holmgren[as], D. Holthuizen[ad], P.F. Honore[f], J.E. Hooper[ab], M. Houlden[u], J. Hrubec[ay],
K. Huet[b], P.O. Hulth[as], K. Hultqvist[as], P. Ioannou[c], P-S. Iversen[d], J.N. Jackson[u], P. Jalocha[p],

G. Jarlskog [w], P. Jarry [am], B. Jean-Marie [r], E.K. Johansson [as], D. Johnson [u], M. Jonker [g],
L. Jonsson [w], P. Juillot [h], G. Kalkanis [c], G. Kalmus [ak], F. Kapusta [v], M. Karlsson [g], E. Karvelas [i],
S. Katsanevas [c], E.C. Katsoufis [ae], R. Keranen [g], J. Kesteman [b], B.A. Khomenko [n],
N.N. Khovanski [n], B. King [u], N.J. Kjaer [g], H. Klein [g], A. Klovning [d], P. Kluit [ad],
A. Koch-Mehrin [ba], J.H. Koehne [o], B. Koene [ad], P. Kokkinias [i], M. Koratzinos [af], K. Korcyl [p],
A.V. Korytov [n], V. Kostioukhine [aq], C. Kourkoumelis [c], O. Kouznetsov [n], P.H. Kramer [ba],
C. Kreuter [o], J. Krolikowski [az], I. Kronkvist [w], U. Kruener-Marquis [ba], W. Kucewicz [p],
K. Kulka [av], K. Kurvinen [m], C. Lacasta [aw], C. Lambropoulos [i], J.W. Lamsa [a], L. Lanceri [au],
V. Lapin [aq], J-P. Laugier [am], R. Lauhakangas [m], G. Leder [ay], F. Ledroit [ℓ], R. Leitner [ac],
Y. Lemoigne [am], J. Lemonne [b], G. Lenzen [ba], V. Lepeltier [r], T. Lesiak [p], J.M. Levy [h], E. Lieb [ba],
D. Liko [ay], J. Lindgren [m], R. Lindner [ba], A. Lipniacka [az], I. Lippi [ai], B. Loerstad [w], M. Lokajicek [j],
J.G. Loken [ah], A. Lopez-Fernandez [g], M.A. Lopez Aguera [ap], M. Los [ad], D. Loukas [i],
J.J. Lozano [aw], P. Lutz [f], L. Lyons [ah], G. Maehlum [af], J. Maillard [f], A. Maio [t], A. Maltezos [i],
F. Mandl [ay], J. Marco [ap], M. Margoni [ai], J-C. Marin [g], A. Markou [i], T. Maron [ba], S. Marti [aw],
F. Matorras [ap], C. Matteuzzi [aa], G. Matthiae [aℓ], M. Mazzucato [ai], M. Mc Cubbin [u], R. Mc Kay [a],
R. Mc Nulty [u], G. Meola [k], C. Meroni [aa], W.T. Meyer [a], M. Michelotto [ai], I. Mikulec [ay],
L. Mirabito [x], W.A. Mitaroff [ay], G.V. Mitselmakher [n], U. Mjoernmark [w], T. Moa [as],
R. Moeller [ab], K. Moenig [g], M.R. Monge [k], P. Morettini [k], H. Mueller [o], W.J. Murray [ak],
G. Myatt [ah], F.L. Navarria [e], P. Negri [aa], R. Nicolaidou [c], B.S. Nielsen [ab], B. Nijjhar [u],
V. Nikolaenko [aq], P.E.S. Nilsen [d], P. Niss [as], A. Nomerotski [ai], V. Obraztsov [aq], A.G. Olshevski [n],
R. Orava [m], A. Ostankov [aq], K. Osterberg [m], A. Ouraou [am], M. Paganoni [aa], R. Pain [v], H. Palka [p],
Th.D. Papadopoulou [ae], L. Pape [g], F. Parodi [k], A. Passeri [ao], M. Pegoraro [ai], J. Pennanen [m],
L. Peralta [t], H. Pernegger [ay], M. Pernicka [ay], A. Perrotta [e], C. Petridou [au], A. Petrolini [k],
F. Pierre [am], M. Pimenta [t], O. Pingot [b], S. Plaszczynski [r], O. Podobrin [o], M.E. Pol [q], G. Polok [p],
P. Poropat [au], V. Pozdniakov [n], P. Privitera [o], A. Pullia [aa], D. Radojicic [ah], S. Ragazzi [aa],
H. Rahmani [ae], P.N. Ratoff [s], A.L. Read [af], P. Rebecchi [g], N.G. Redaelli [aa], M. Regler [ay], D. Reid [g],
P.B. Renton [ah], L.K. Resvanis [c], F. Richard [r], M. Richardson [u], J. Ridky [j], G. Rinaudo [at],
I. Roditi [q], A. Romero [at], I. Roncagliolo [k], P. Ronchese [ai], C. Ronnqvist [m], E.I. Rosenberg [a],
S. Rossi [g], E. Rosso [g], P. Roudeau [r], T. Rovelli [e], W. Ruckstuhl [ad], V. Ruhlmann-Kleider [am],
A. Ruiz [ap], H. Saarikko [m], Y. Sacquin [am], G. Sajot [ℓ], J. Salt [aw], J. Sanchez [y], M. Sannino [k,an],
S. Schael [g], H. Schneider [o], M.A.E. Schyns [ba], G. Sciolla [at], F. Scuri [au], A.M. Segar [ah], A. Seitz [o],
R. Sekulin [ak], M. Sessa [au], G. Sette [k], R. Seufert [o], R.C. Shellard [aj], I. Siccama [ad], P. Siegrist [am],
S. Simonetti [k], F. Simonetto [ai], A.N. Sisakian [n], G. Skjevling [af], G. Smadja [am,x], O. Smirnova [n],
G.R. Smith [ak], R. Sosnowski [az], D. Souza-Santos [aj], T.S. Spassoff [ℓ], E. Spiriti [ao], S. Squarcia [k],
H. Staeck [ba], C. Stanescu [ao], S. Stapnes [af], G. Stavropoulos [i], F. Stichelbaut [b], A. Stocchi [r],
J. Strauss [ay], J. Straver [g], R. Strub [h], B. Stugu [d], M. Szczekowski [g], M. Szeptycka [az],
P. Szymanski [az], T. Tabarelli [aa], O. Tchikilev [aq], G.E. Theodosiou [i], A. Tilquin [z],
J. Timmermans [ad], V.G. Timofeev [n], L.G. Tkatchev [n], T. Todorov [h], D.Z. Toet [ad], O. Toker [m],
B. Tome [t], E. Torassa [at], L. Tortora [ao], D. Treille [g], U. Trevisan [k], W. Trischuk [g], G. Tristram [f],
C. Troncon [aa], A. Tsirou [g], E.N. Tsyganov [n], M-L. Turluer [am], T. Tuuva [m], I.A. Tyapkin [v],
M. Tyndel [ak], S. Tzamarias [u], S. Ueberschaer [ba], O. Ullaland [g], V. Uvarov [aq], G. Valenti [e],
E. Vallazza [at], J.A. Valls Ferrer [aw], C. Vander Velde [b], G.W. Van Apeldoorn [ad], P. Van Dam [ad],
M. Van Der Heijden [ad], W.K. Van Doninck [b], P. Vaz [g], G. Vegni [aa], L. Ventura [ai], W. Venus [ak],
F. Verbeure [b], M. Verlato [ai], L.S. Vertogradov [n], D. Vilanova [am], P. Vincent [x], L. Vitale [m],
E. Vlasov [aq], A.S. Vodopyanov [n], M. Vollmer [ba], M. Voutilainen [m], V. Vrba [ao], H. Wahlen [ba],
C. Walck [as], F. Waldner [au], A. Wehr [ba], M. Weierstall [ba], P. Weilhammer [g], J. Werner [ba],
A.M. Wetherell [g], J.H. Wickens [b], G.R. Wilkinson [ah], W.S.C. Williams [ah], M. Winter [h],

M. Witek [p], G. Wormser [r], K. Woschnagg [av], N. Yamdagni [as], P. Yepes [g], A. Zaitsev [aq],
A. Zalewska [p], P. Zalewski [r], D. Zavrtanik [ar], E. Zevgolatakos [i], G. Zhang [ba], N.I. Zimin [n],
M. Zito [am], R. Zuberi [ah], R. Zukanovich Funchal [f], G. Zumerle [ai] and J. Zuniga [aw]

[a] Ames Laboratory and Department of Physics, Iowa State University, Ames IA 50011, USA
[b] Physics Department, Universitaire Instelling Antwerpen, Universiteitsplein 1, B-2610 Wilrijk, Belgium
and IIHE, ULB-VUB, Pleinlaan 2, B-1050 Brussels, Belgium
and Faculté des Sciences, Université de l'Etat Mons, Av. Maistriau 19, B-7000 Mons, Belgium
[c] Physics Laboratory, University of Athens, Solonos Street 104, GR-10680 Athens, Greece
[d] Department of Physics, University of Bergen, Allégaten 55, N-5007 Bergen, Norway
[e] Dipartimento di Fisica, Università di Bologna and INFN, Via Irnerio 46, I-40126 Bologna, Italy
[f] Collège de France, Laboratoire de Physique Corpusculaire, IN2P3–CNRS, F-75231 Paris Cedex 05, France
[g] CERN, CH-1211 Geneva 23, Switzerland
[h] Centre de Recherche Nucléaire, IN2P3–CNRS/ULP, B.P. 20, F-67037 Strasbourg Cedex, France
[i] Institute of Nuclear Physics, NCSR Demokritos, P.O. Box 60228, GR-15310 Athens, Greece
[j] FZU, Institute of Physics of the C.A.S. High Energy Physics Division,
Na Slovance 2, CS-180 40, Praha 8, Czech Republic
[k] Dipartimento di Fisica, Università di Genova and INFN, Via Dodecaneso 33, I-16146 Genova, Italy
[ℓ] Institut des Sciences Nucléaires, IN2P3–CNRS, Université de Grenoble 1, F-38026 Grenoble, France
[m] Research Institute for High Energy Physics, SEFT, Siltavuorenpenger 20 C, SF-00170 Helsinki, Finland
[n] Joint Institute for Nuclear Research, Dubna, Head Post Office, P.O. Box 79, 101 000 Moscow, Russian Federation
[o] Institut für Experimentelle Kernphysik, Universität Karlsruhe, Pf. 6980, D-7500 Karlsruhe 1, Germany
[p] High Energy Physics Laboratory, Institute of Nuclear Physics, Ul. Kawiory 26 a, PL-30055 Krakow 30, Poland
[q] Centro Brasileiro de Pesquisas Fisicas, rua Xavier Sigaud 150, RJ-22290 Rio de Janeiro, Brazil
[r] Université de Paris-Sud, Laboratoire de l'Accélérateur Linéaire, IN2P3–CNRS, Bâtiment 200, F-91405 Orsay, France
[s] School of Physics and Materials, University of Lancaster, GB - Lancaster LA1 4YB, UK
[t] LIP, IST, FCUL, Av. Elias Garcia, 14 - 1o, P-1000 Lisboa Codex, Portugal
[u] Department of Physics, University of Liverpool, P.O. Box 147, GB - Liverpool L69 3BX, UK
[v] LPNHE, IN2P3–CNRS, Universités Paris VI et VII, Tour 33 (RdC), 4 place Jussieu, F-75252 Paris Cedex 05, France
[w] Department of Physics, University of Lund, Sölvegatan 14, S-22363 Lund, Sweden
[x] Université Claude Bernard de Lyon, IPNL, IN2P3–CNRS, F-69622 Villeurbanne Cedex, France
[y] Universidad Complutense, Avda. Complutense s/n, E-28040 Madrid, Spain
[z] Université d'Aix – Marseille II – CPP, IN2P3–CNRS, F-13288 Marseille Cedex 09, France
[aa] Dipartimento di Fisica, Università di Milano and INFN, Via Celoria 16, I-20133 Milan, Italy
[ab] Niels Bohr Institute, Blegdamsvej 17, DK-2100 Copenhagen Ø, Denmark
[ac] NC, Nuclear Centre of MFF, Charles University, Areal MFF, V Holesovickach 2, CS-180 00, Praha 8, Czech Republic
[ad] NIKHEF-H, Postbus 41882, NL-1009 DB Amsterdam, The Netherlands
[ae] National Technical University, Physics Department, Zografou Campus, GR-15773 Athens, Greece
[af] Physics Department, University of Oslo, Blindern, N-1000 Oslo 3, Norway
[ag] Departamento Fisica, Universidad Oviedo, C/P.Jimenez Casas, S/N-33006 Oviedo, Spain
[ah] Department of Physics, University of Oxford, Keble Road, Oxford OX1 3RH, UK
[ai] Dipartimento di Fisica, Università di Padova and INFN, Via Marzolo 8, I-35131 Padua, Italy
[aj] Departamento de Fisica, Pontificia Universidade Católica, C.P. 38071, RJ-22453 Rio de Janeiro, Brazil
[ak] Rutherford Appleton Laboratory, Chilton, GB - Didcot OX11 0QX, UK
[aℓ] Dipartimento di Fisica, Università di Roma II and INFN, Tor Vergata, I-00173 Rome, Italy
[am] Centre d'Etude de Saclay, DSM/DAPNIA, F-91191 Gif-sur-Yvette Cedex, France
[an] Dipartimento di Fisica, Università di Salerno, I-84100 Salerno, Italy
[ao] Istituto Superiore di Sanità, INFN, Viale Regina Elena 299, I-00161 Rome, Italy
[ap] CEAFM, CSIC, Universidad Cantabria, Avda. los Castros, S/N-39006 Santander, Spain
[aq] Institute for High Energy Physics, Serpukov, P.O. Box 35, Protvino (Moscow Region), Russian Federation
[ar] J. Stefan Institute and Department of Physics, University of Ljubljana, Jamova 39, SI-61000 Ljubljana, Slovenia
[as] Fysikum, Stockholm University, Box 6730, S-113 85 Stockholm, Sweden
[at] Dipartimento di Fisica Sperimentale, Università di Torino and INFN, Via P. Giuria 1, I-10125 Turin, Italy
[au] Dipartimento di Fisica, Università di Trieste and INFN, Via A. Valerio 2, I-34127 Trieste, Italy
and Istituto di Fisica, Università di Udine, I-33100 Udine, Italy
[av] Department of Radiation Sciences, University of Uppsala, P.O. Box 535, S-751 21 Uppsala, Sweden

aw IFIC, Valencia–CSIC, and DFAMN, Universidad de Valencia,
Avda. Dr. Moliner 50, E-46100 Burjassot (Valencia), Spain

ay Institut für Hochenergiephysik, Österreichische Akademie der Wissenschaften,
Nikolsdorfergasse 18, A-1050 Vienna, Austria

az Institute of Nuclear Studies and University of Warsaw, Ul. Hoza 69, PL-00681 Warsaw, Poland

ba Fachbereich Physik, Universität Wuppertal, Pf. 100 127, D-5600 Wuppertal 1, Germany

Evidence for the production of b-flavoured baryons in Z^0 decays is reported from the analysis of 365 000 hadronic events collected by the DELPHI detector. Assuming that most of the weakly decaying b flavoured baryons produced by the Z^0 are Λ_b, the observed signal of $(\Lambda l^- + \overline{\Lambda} l^+)$ pairs, where l is a high transverse momentum lepton in the same jet as the Λ, leads to a production rate: $f(b \to \Lambda_b) \times \mathrm{Br}(\Lambda_b \to \Lambda l \nu X) = (0.41 \pm 0.13 \pm 0.09)\%$. Using a sample of 18 reconstructed Λ_b decay vertices, the lifetime is determined to be $\tau(\Lambda_b) = (1.04^{+0.48}_{-0.38} \pm 0.10)$ ps.

1. Introduction

Although b physics has been studied for more than a decade, little is known about the spectroscopy of hadrons containing b quarks. This is particularly true for baryons, which have a rather small production rate. It is only recently that the first quantitative results appeared from high energy colliders such as the Sp$\overline{\text{p}}$S [1] and LEP [2,3]. The Λ_b, made of the u, d and b quarks, is believed to be the lightest baryon involving the b quark. Its study will provide data on the fragmentation of the b quark into baryons and its subsequent weak decays.

LEP running at the Z^0 peak is well suited for this experimental program. The high $Z^0 \to$ hadrons cross-section and the large branching fraction to $b\overline{b}$ pairs provide large numbers of b-hadrons. The hard fragmentation of b quarks ensures that the b-hadrons have high momenta and therefore travel a measurable distance before decaying.

In a given jet an energetic lepton with a high transverse momentum (p_T) to the jet axis and an energetic Λ with baryon number opposite to the charge of the lepton (that is Λl^- and $\overline{\Lambda} l^+$ pairs[#1], the so-called *right sign pairs*), signal a Λ_b candidate. Assuming the semileptonic decay of the Λ_b proceeds through the $b \to c \to s$ quark decay chain (the ud diquark pair is just a spectator) the negative lepton appears from

---

[#1] Although from now on only Λl^- pairs will be mentioned explicitly, reference to the charge conjugate combinations will always be implied.

the $b \to c$ part of the process and the Λ appears at the end of the decay chain. The kinematics of the $b \to c \to s$ decay chain impart a high momentum to the Λ, while the $b \to c$ decay gives a high longitudinal and transverse momentum lepton. Other b-baryons, the Ξ_b and the Ω_b in particular, can also lead to the same final state, but their production is suppressed due to the need to create one or two $s\overline{s}$ pairs. The Σ_b, on the other hand, is expected to decay via strong or electromagnetic interactions to the Λ_b [4]. Under these assumptions right sign Λl pairs single out Λ_b production. Other Λl producing processes surviving the selection cuts discussed in the paper do not exhibit any sign correlation and can be eliminated by subtraction of the wrong sign pair distributions.

In the following sections the detector and the event selection procedure, the lepton and Λ identification algorithms and the method of extracting the Λl combinations from the data are described. Assuming b-baryon production is dominated by the Λ_b, the observed rate is translated into a measurement of the product branching ratio: $\Gamma_{b\overline{b}}/\Gamma_{\text{had}} \times f(b \to \Lambda_b) \times \mathrm{Br}(\Lambda_b \to \Lambda l \nu X)$, where $f(b \to \Lambda_b)$ is the probability that a b-quark fragments to a Λ_b. Finally a clean sample of $\Lambda\mu$ events is used to determine the Λ_b lifetime.

2. The DELPHI detector

The DELPHI detector has been described in detail elsewhere [5]. Relevant to this analysis are the tracking detectors and, for lepton identification, the

calorimeters and the muon chambers.

The tracking detectors, immersed in a 1.23 T magnetic field, are the microvertex detector (VD), the inner detector (ID), the time projection chamber (TPC), the outer detector (OD) and the forward chambers FCA and FCB in the end-caps. Using the ID, TPC and OD, the momentum resolution is $\sigma(p)/p = 0.0015p$ where p is expressed in GeV/c. The silicon microvertex detector is made of three layers at radii 6.3, 9 and 11 cm (only the last two were operational in 1990 data taking) each providing $r\phi$ readout. With the microvertex detector hits included in the track fits, a precision of 30 μm is achieved in the plane transverse to the beam on extrapolating tracks of high momentum particles to the primary interaction point and a momentum resolution of 3.5% for a 45.5 GeV/c muon is obtained. The TPC provides up to 16 space points, in a volume enclosed by two cylinders of 2.7 m length and radii 30 and 122 cm, for charged particle tracks with polar angles between 39° and 141°. It also provides a measurement of the mean ionisation (dE/dX) from 192 sense wires. For isolated particles (muons in di-muon events) the RMS resolution on the mean dE/dX is 5.5%, while for particles in jets the RMS resolution is 7.5%. The two track resolution being 1.5 cm, it is difficult to determine the dE/dX for 25% of the charged particles that overlap within this distance along more than half of the TPC radial range.

In the polar angle range $10° < \theta < 170°$ muon detection is provided by layers of drift chambers in the barrel and end-cap regions. The first layer is sited inside the iron return yoke after 90 cm of iron and the second is placed outside (after 1 m of iron). In the barrel region ($50° < \theta < 130°$) there is a third layer of chambers to provide full coverage in azimuthal angle (ϕ).

Electromagnetic showers in the barrel region ($44° < \theta < 136°$) are detected by the high density projection chamber, HPC, with nine layers of longitudinal segmentation (18 radiation lengths in total) and a granularity of 1° in ϕ.

3. Hadronic event selection

The data samples taken in 1990 and 1991 amount to integrated luminosities of 5.6 pb^{-1} and 10.7 pb^{-1}

respectively. The trigger for multi-hadron events was more than 99% efficient. For hadronic event selection, a charged particle is retained if its momentum (p) is between 0.1 and 50 GeV/c, $\sigma(p)/p$ is below 100%, its measured path length is longer than 20 cm, and its distance of closest approach to the nominal interaction point is less than 4 cm in the plane transverse to the beams (see section 4.3 for cuts applied to charged tracks used in the search for Λs) and less than 10 cm along the beam. An event is accepted as hadronic if it has more than five such tracks and a total energy carried by charged particles (computed assuming all are pions) greater than 0.12 $\sqrt{s}$. A total of 120 000 and 245 000 hadronic events were selected by these criteria from the 1990 and 1991 data samples, respectively. The efficiency of the hadronic event selection is $(94.7 \pm 0.4)\%$ [6].

Well measured ($\sigma(p)/p < 10\%$) charged tracks in these events are clustered into jets using the LUND jet finding algorithm (routine LUCLUS) [7] with a clustering mass parameter equal to 6.5 GeV/c^2.

4. Lepton and Λ identification

4.1. Muon selection

For the analysis of $\mu\Lambda$ pairs, the hadronic data sample in which the TPC and the barrel and forward muon chambers were operational has been used; this requirement restricts the sample to 323 000 Z^0 hadronic decays.

As explained in detail in refs. [8,9], charged tracks with momenta above 3 GeV/c are extrapolated to the muon chambers and matched to track elements measured in these chambers. A muon candidate is used in the analysis if it is in the polar angle region $20° < \theta < 160°$. The muon identification efficiency is $(78 \pm 2)\%$. The probability for a hadron to fake a muon by punching through or decaying in flight has been studied using the hadron calorimeter and estimated to be $(0.94 \pm 0.10)\%$. A total of 28 849 hadronic events are found with a muon candidate. Of the muons with transverse momentum p_T greater than 1 GeV/c with respect to their jet axis, 54% are estimated to come from direct b quark decay [9].

4.2. Electron selection

The electron sample has been extracted from the hadronic data in which the TPC and the HPC were operational; this sample amounts to 329 000 Z^0 hadronic decays.

As explained in refs. [9,10], charged tracks with momenta above 3 GeV/c are extrapolated to the HPC and matched to the energy depositions measured. A charged particle is identified as an electron if the energy deposition in all nine layers of the HPC and the dE/dX in the TPC are consistent with expectation. From the measured energies in the nine HPC layers a χ^2 is determined relative to the values expected for an electron of the given momentum. The particle is accepted as an electron if the χ^2-probability is greater than 3% and the dE/dX if measured is greater than 1.42 times the minimum ionisation. Only electron candidates in the polar angle range $46° < \theta < 134°$ are used in the analysis. With the above criteria the electron identification efficiency is determined to be $(45 \pm 3)\%$. The probability for hadrons to fake a prompt electron is determined to be $(0.90 \pm 0.04)\%$ from a sample of pions from reconstructed neutral kaon decays.

The final sample of hadronic events with an electron candidate amounts to 26 394 events. Many of these electron candidates originate from gamma conversions before the calorimeter; however, they are found to have a much lower mean p_T with respect to the jet axis than prompt electrons. For p_T greater than 1 GeV/c, 38% of the electron candidates are estimated to come from direct b quark decay [9].

4.3. Λ selection

The search for the $\Lambda \rightarrow p\pi^-$ decays in hadronic events with an identified lepton has been performed by fitting to a common secondary vertex pairs of oppositely charged tracks with a total momentum below 40 GeV/c. Candidate secondary vertices are accepted if

(i) the distance from the primary vertex is less than 80 cm in the plane transverse to the beam;

(ii) the χ^2 probability is greater than 1%; and

(iii) their separation in x and y from the average beam spot (calculated for each LEP fill) is more than four times the relevant error (typically 300 μm).

Besides these requirements a Λ candidate has to satisfy the following conditions:

– the angle, in the plane transverse to the beam axis, between the $(p\pi)$ momentum direction and the vector joining the primary and secondary vertices is less than 1.5°;

– the distance of closest approach of the Λ trajectory to the primary vertex of the event is less than 4 mm in the plane perpendicular to the beam;

– $\cos\theta_p^* > -0.94$ where θ_p^* is the angle between the proton and the Λ line of flight in the Λ rest frame;

– the invariant mass of the two particles, when each is assumed to be a pion, is inconsistent with that of a neutral kaon (i.e. outside the interval $0.485 < M(\pi^+\pi^-) < 0.515$ GeV/c^2);

– the innermost hits for each track in the pair are consistent with the measured transverse decay length of the candidate;

– both decay products have a p_T with respect to the Λ line of flight greater than 30 MeV/c; this cut reduces the background from gamma conversions to almost zero;

– the apparent lifetime of the Λ exceeds 0.02 ns (cf. $\tau_\Lambda = 0.26$ ns);

– the dE/dX of the assumed pion and proton tracks are either unmeasured or match the expected values within 3.5 standard deviations.

The $p\pi$ invariant mass spectrum for 4052 secondary vertex candidates surviving the above cuts and having momenta above 4 GeV/c is shown in fig. 1. A fit of a Gaussian curve on the top of a polynomial background to this distribution gives 527 ± 29 $\Lambda \rightarrow p\pi^-$ decays with a central value of 1115.9 ± 0.3 MeV/c^2 for the Λ mass and a resolution of 3.7 ± 0.3 MeV/c^2.

4.4. Comparison of data and Monte Carlo samples

The effect of the cuts described above was studied with a sample of 25 000 Monte Carlo hadronic events containing a tagged muon (identified by using the same algorithm as in the data). Events were generated with the LUND Parton Shower model with a b fragmentation function that reproduces the lepton momentum spectrum observed in semi-leptonic b-decays [6]. In the Monte Carlo, 10% of the b quarks lead to a Λ_b when the decays of the heavier b-baryons via pion emission are included. Ξ_b and Ω_b production rates are respectively lower by one and two orders of
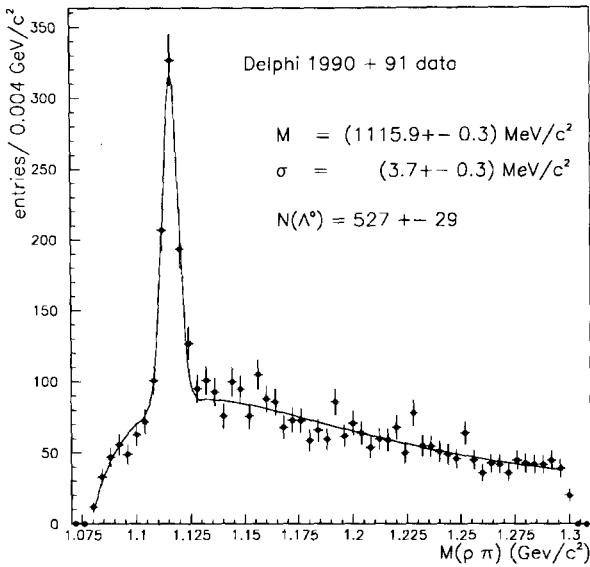
Fig. 1. Distribution of $p\pi$ invariant mass in the data for Λ with 4 GeV in Z^0 hadronic events tagged by a lepton.

magnitude. The events were passed through the complete DELPHI detector simulation program [11] and reconstructed and analysed with the same programs as those for the data.

The mean efficiency to select the $\Lambda \to p\pi^-$ decays for momenta greater than 4 GeV/c is estimated to be $(16.2 \pm 2.4(\text{syst.})\%)$ in the Monte Carlo, which correctly reproduces the observed Λ spectrum. Sources of systematic error on the Λ reconstruction efficiency are the track efficiency for the Λ decay products, the selection efficiency of the cuts, the modelling of the quark fragmentation and limited statistics in the Monte Carlo. The relatively low efficiency detecting a high momentum Λ is mainly due to the small outer radius of the TPC, which makes it difficult to separate the decay prongs of an energetic Λ.

5. Λl associated production

To enrich the Λ_b content in the sample of events containing a Λ and an associated lepton in the same jet, a series of cuts have been devised from a study of the Monte Carlo hadronic events and from a dedicated Monte Carlo simulation of 10 000 events in the channel $b\bar{b} \to \Lambda_b X \to \Lambda_c l \nu X$, generated by the

LUND event generator with the fragmentation function mentioned above.

To reduce the Λ background from light quark fragmentation processes, which mainly contribute to the low momentum region, only Λ candidates with momentum greater than 4 GeV/c have been considered for the correlation search. The b-baryon decay candidates selected from this sample are those with the Λ within a cone of 1 radian half angle around the lepton track.

The momentum cut keeps 85% of the Λs coming from Λ_b decay.

Sources of Λl pairs originating from non-Λ_b events include the following three classes, in order of decreasing importance:

(i) Accidental combinations. This class includes
– random association of a Λ from fragmentation, surviving the Λ momentum cut, and a lepton from a heavy flavour decay,
– associations of a Λ and a fake lepton.

(ii) The semileptonic Λ_c decays (either from $c\bar{c}$ events or from cascades after $b \to c$ decays).

(iii) The semileptonic B meson decays: $\bar{B} \to \Lambda_c^+ \bar{N} l^- \bar{\nu} X$, where $\bar{N}$ is an antibaryon.

Background from accidental pairs of a Λ with a fake lepton is expected to contribute identically to both right sign and wrong sign combinations when the misidentified lepton is a pion; this is not true if the fake lepton is a proton or a kaon, due to baryonic number and strangeness local conservation in the hadronization. However, the study of the Monte Carlo hadronic events shows that this effect is negligible for high p_T tracks. In the Λ–antiproton case, this is confirmed by the data: by determining the number of protons from the Λ sample shown in fig. 1 which are misidentified as leptons, an upper limit of 0.8 events in the right sign pairs is derived, under the assumption that the Λ and antiproton spectrum are similar. The case of a Λ produced in the fragmentation of a quark (particularly a heavy quark) associated with a genuine lepton can also lead to different contributions in the right and wrong sign combinations, and will be discussed below. Finally, events from class 2 contribute only wrong sign pairs, while class 3 gives right sign combinations; both processes have the p_T spectrum of the lepton significantly softer than the one in the Λ_b decay.

To reduce these backgrounds it is required that

Table 1
Expected number of detected Λs selected by the cuts in 300 000 $q\bar{q}$ MC events.

Cut	All Λ	Λ from Λ_b decays
none	13700	68
$p_L > 4$ GeV/c	5560	58
$p_l > 3$ GeV/c	250	43
$(p_T)_l > 1$ GeV/c	127	37
$M(\Lambda l) > 2.3$ GeV/c^2	86	33

Fig. 2. Distribution of pπ invariant mass for Λl correlations in the data: (a) right sign combinations; (b) wrong sign combinations. The shaded area corresponds to Λ–electron combinations. The arrows show the invariant mass range considered in the text.

– $(p_T)_l > 1$ GeV/c where p_T is computed with respect to the jet axis after the lepton has been subtracted from the jet. Semileptonic decays of Λ_c and $\bar{B}$ decays are suppressed (approximately 27% of each survive this cut and the momentum cut in the lepton selection, while 66% of the Λ_b are accepted).

– $2.3 \leqslant M(\Lambda l) < 6.0$ GeV/c^2 where $M(\Lambda l)$ is the invariant mass of the Λ and the lepton. Again Λ_c and $\bar{B}$ semileptonic decays are preferentially removed (only 5% of Λ_c and 15% of $\bar{B}$ semileptonic decays surviving the $(p_T)_l$ cut remain) while 88% of the Λ_bs are retained.

The effectiveness of the various cuts used in the analysis is indicated in table 1 where the numbers of Λ surviving each sequential cut is shown for a sample of 300 000 $q\bar{q}$ Monte Carlo events. Also the expected number of events from Λ_b decays assuming a production rate $f(b \to \Lambda_b) \times \mathrm{Br}(\Lambda_b \to \Lambda l \nu X) = 0.5\%$ is indicated.

To study the effect of accidental pairing of a genuine Λ and a lepton at the generation level, a sample of 10^6 Z^0 events was generated with the Lund Jetset 7.2 program with default parameters and the first three cuts of table 1 applied. The (Λl) invariant mass distributions for the right sign pairs in events with no b-baryon and for wrong sign combinations from all sources were compared: the ratio between right sign Λl pairs and wrong sign ones with $M(\Lambda l) > 2.3$ GeV/c^2 is 0.8. However, it can rise up to 1.2 depending on the assumed yield of baryon–antibaryon pairs accompanying a B-meson in the fragmentation of a b quark. In the following analysis it is assumed that this background is identical in right and wrong sign combinations within a systematic error of $\pm 20\%$.

The $(p\pi)$ invariant mass distributions obtained in the data after the cuts discussed above for the right
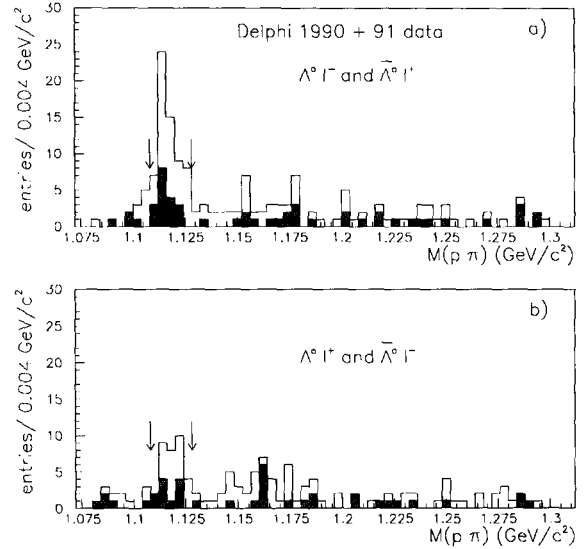
and wrong sign combinations are shown in figs. 2a and 2b respectively[#2]. The signal of (22 ± 5) events in fig. 2b is thus interpreted as the remaining background of accidental combinations of wrong sign Λ–lepton pairs (the lepton being either a genuine one or a misidentified pion). Following the above discussion, the same background contribution is expected to the Λ peak in the distribution of right sign pairs visible in fig. 2a.

From these distributions it is clear that there is an excess of 30 ± 10 events (23 ± 8 and 7 ± 5 events in the muon and electron samples respectively) in the right sign combination in the $(p\pi)$ invariant mass range $1.108 \leqslant M_{p\pi} < 1.128$ GeV/c^2. The corresponding Λ and lepton momentum distributions and the Λ–lepton invariant mass distribution, obtained by subtracting the wrong sign distributions from the right sign ones, are shown in fig. 3 together with the Monte Carlo prediction, normalized to the data, from the dedicated

[#2] The probability for a right sign combination to become a wrong sign one is dominated by the probability to fake the charge of the lepton (the baryonic number of the Λ is correctly measured when the vertex fit is successful) and it is negligible in the momentum region below 20 GeV.
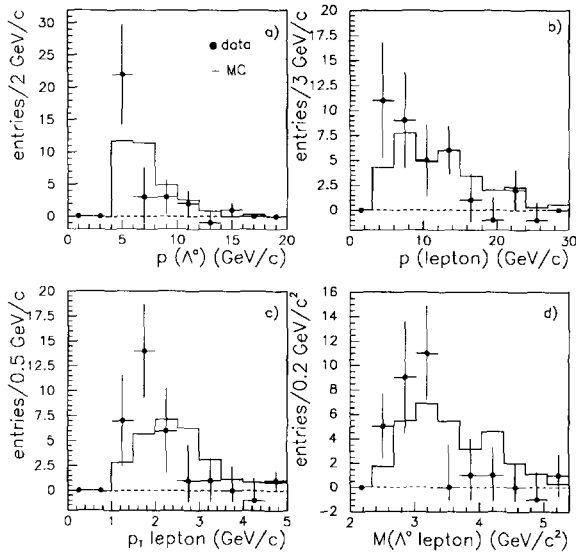
Fig. 3. Distribution for some kinematical variables (background subtracted) for the right sign combinations.

Λ_b generation. Within the low statistics, the agreement is fair.

6. Λ_b production rate

To determine the Λ_b production rate the remaining background in the sample of Λl selected events has to be evaluated.

Semileptonic decays of the Λ_c contribute an estimated 0.4 events to wrong sign combinations. This comes from the total selection efficiency for this channel of $(0.1 \pm 0.03)\%$, using a 10% probability for a c quark to hadronise to a Λ_c, a 20% probability for a b quark to produce a Λ_c, and the $\Lambda_c^+ \rightarrow \Lambda e^+ X$ branching ratio of $(1.2 \pm 0.4)\%$ [12].

Background right sign combinations can come from class 3 events. The number of background events from semileptonic B-meson decays with a Λ in the final state is estimated to be less than 0.1 on the assumption that a b quark hadronises to a B-meson 100% of the time. This is determined from the selection efficiency of $(0.3 \pm 0.1)\%$, using the ARGUS upper limit at 90% confidence level for $\mathrm{Br}(\overline{B} \rightarrow p\ell^-\nu X) = 1.6 \times 10^{-3}$ [13] and the CLEO assertion that 30% of the protons produced in B decays come from Λ decays [14].

As discussed in the previous section, it is assumed that background from other sources contributes equally to the right and wrong sign combinations within a 20% uncertainty and thus is removed by the subtraction. Due to this uncertainty, a systematic error of ± 4.4 events (i.e. 20% of the observed signal of 22 ± 5 events in the wrong combinations plot, see fig. 2b) is added in quadrature to the other systematic errors.

In summary, the observed excess of 30 ± 10 events is a statistically significant signal of Λ_b. From this excess the product branching ratio $\mathrm{BR} = \Gamma_{b\bar{b}}/\Gamma_{\mathrm{had}} \times f(b \rightarrow \Lambda_b) \times \mathrm{Br}(\Lambda_b \rightarrow \Lambda l\nu X)$ is determined. The total efficiency, including the $\Lambda \rightarrow p\pi^-$ branching ratio and the geometrical acceptance for lepton detection, is $(3.4 \pm 0.8\%)$ for the muon channel and $(1.3 \pm 0.4\%)$ for the electron channel. The systematic errors include the uncertainties in the Λ reconstruction and lepton identification efficiencies and in the Λ and lepton spectrum from the Λ_b decay. From the selected samples of Z^0 hadronic decays defined above,

$$\mathrm{BR} = 0.99 \pm 0.33 \pm 0.26 \times 10^{-3}$$

for the $\Lambda\mu$ sample,

and

$$\mathrm{BR} = 0.76 \pm 0.54 \pm 0.24 \times 10^{-3}$$

for the Λe sample.

Assuming lepton universality and using our measured value of $\Gamma_{b\bar{b}}/\Gamma_{\mathrm{had}} = 0.219 \pm 0.014 \pm 0.019$ [15], the product $f(b \rightarrow \Lambda_b) \times \mathrm{Br}(\Lambda_b \rightarrow \Lambda l\nu X)$ is determined to be $(0.41 \pm 0.13 \pm 0.09\%)$ per lepton flavour, compatible with values from other LEP experiments [2,3].

7. Λ_b lifetime

The vertex reconstruction of semi-exclusive decays has proved to be a powerful method in determining the B-mesons lifetimes [16]. The same approach is used for Λ_b lifetime determination by reconstructing secondary vertices with the Λ, the correlated high p_T

muon [#3] and an opposite charged track (supposed
to be a pion) with momentum greater than 0.6 GeV
and with associated hits in the microvertex detector.
This procedure selects Λ_b events in which the follow-
ing Λ_c has a decay length within the resolution of the
vertex reconstruction (300 μm), but does not intro-
duce any bias in the length distribution of the original
Λ_b. This has been checked in the simulation, where
the reconstructed and generated Λ_b lifetimes are in
good agreement. To reduce the combinatorial back-
ground, the ($\mu\Lambda\pi$) invariant mass is required to be
less than 5.6 GeV and the ($\Lambda\pi$) invariant mass to be
less than 2.4 GeV. Further, the vertex fit probability
has to be greater than 1%. In case of more than one
reconstructed vertex, the one with highest probability
is chosen. In the simulation, it is found that the effi-
ciency for the Λ_b decay vertex reconstruction is about
50%, independent of the Λ_b lifetime, and in 90% of
the reconstructed decays the pion attached to the ver-
tex does originate from the Λ_b decay chain. The error
on the primary vertex (50 μm), reconctructed event
by event with the beam spot constraint, is included
in the decay length error and does not introduce any
systematic effect.

The Λ_b momentum estimation required to compute
the lifetime from the measured decay length is ob-
tained by the "residual-energy" technique. The resid-
ual energy is computed by subtracting the energy asso-
ciated to the Λ_b candidate (the Λ, lepton and pion en-
ergy) from the total energy associated to charged par-
ticles in the lepton hemisphere. The Λ_b energy is then
estimated by subtracting this residual energy from
the beam energy. Events with badly measured tracks
in the hemisphere with unphysical reconstructed mo-
mentum are not considered for the lifetime determi-
nation [#4]. The method is affected by two main sources
of systematic error. The energy associated to all the
neutral particles in the hemisphere is by definition in-
cluded in the Λ_b energy. On the other hand, charged pi-
ons from the Λ_b decay chain may be wrongly included
in the residual energy computation. The Monte Carlo
study shows that the two effects nearly compensate,
the correction factor to reproduce the generated Λ_b

spectrum being on average 0.97 ± 0.02. The resolution
obtained for the Λ_b momentum is 8%. The systematic
error on the correction factor includes the statistical
error of the Monte Carlo and the uncertainty on the
b-fragmentation function. The Λ_b mass was taken to
be 5.62 GeV with an uncertainty of $\pm$ 200 MeV which
directly contributes to the systematic error.

For the lifetime analysis the 1991 muon data (with
all the three layers of the microvertex operational)
were used; out of 37 right sign $\Lambda\mu$ events, 18 decays
were reconstructed. From a fit to the mass plots for
the right and wrong sign correlations, the Λ_b content
of this sample is determined to be (63 $\pm$ 10%). Back-
ground events come from secondary vertices originat-
ing from charm and B-mesons decays, whose average
lifetime will be determined by the data (see below),
and from fake vertices whose lifetime distribution has
zero average value. The first component is assumed
to be (66 $\pm$ 4%) of the background (54% from direct
$b \rightarrow \mu X$ and 12% from cascade $b \rightarrow c \rightarrow \mu$ decays),
in agreement with the known b-purity of the high p_T
muon sample [9]. Its average lifetime is determined
from a larger sample of decays reconstructed in the
high p_T muon events using the same vertex finding
algorithm and all the V^0 candidates with momentum
greater than 3 GeV and ($p\pi$) invariant mass less than
1.3 GeV. Since the length distribution of the recon-
structed vertices is dominated by the measurement of
the charged tracks (although including the Λ in the fit
has an important role in reducing the combinatorial
background), it is not modified by the presence of a
fake V^0 instead of a true one. The second component
is assumed to have a gaussian spread determined by
the detector resolution.

A maximum likelihood fit was performed to the
lifetime distribution of the 18 decays of the Λ_b sample
and to the one of the background vertices described
above, with the likelihood function [16]

$$L = -\sum_i \log[f(t_i, \sigma_i, \tau, \tau_B)],$$

with

[#3] The extrapolation of the electron track is not precise
enough for this study, due to bremsstrahlung effects.

[#4] Such events were kept in the analysis of ref. [16], and
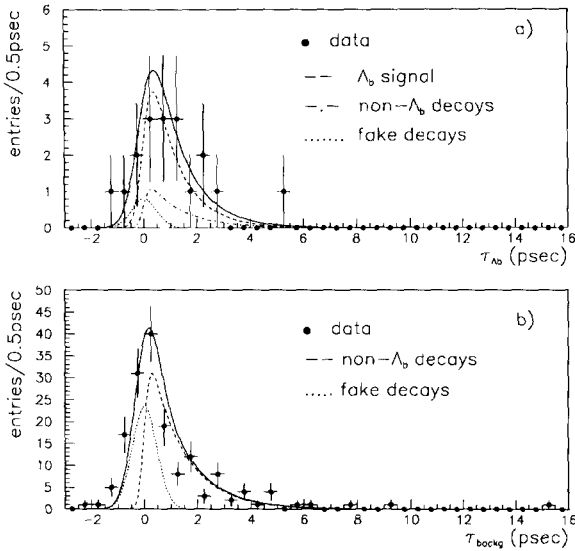this led to a larger estimate of the systematic uncertainty.

Fig. 4. Lifetime distribution for (a) the Λ_b sample and for (b) the background sample.

$$f(t_i, \sigma_i, \tau, \tau_B)$$

$$= N_s \exp(\sigma_i^2/2\tau^2 - t_i/\tau)$$

$$\times \operatorname{erfc}[(\sigma_i/\tau - t_i/\sigma_i)/\sqrt{2}]/2\tau$$

$$+ N_{fb} \exp(\sigma_i^2/2\tau_B^2 - t_i/\tau_B)$$

$$\times \operatorname{erfc}[(\sigma_i/\tau_B - t_i/\sigma_i)/\sqrt{2}]/2\tau_B$$

$$+ N_b \exp(-t_i^2/2\sigma_i^2),$$

where τ and τ_B are the signal and background lifetimes; σ_i is the error on the measured decay time, t_i, the normalization constants for the signal, the background from non Λ_b decays and fake vertices (N_s, N_{fb} and N_b respectively) were fixed in the fit using the values of the purity and background composition discussed above. The two lifetime distributions and the probability functions resulting from the fit are shown in fig. 4 and the two mean lifetimes are determined to be

$$\tau_B = 1.28^{+0.15}_{-0.17} \text{ ps}$$

and

$$\tau(\Lambda_b) = 1.04^{+0.48}_{-0.38} \text{ ps}.$$

Table 2
Contributions to the systematic error on the Λ_b lifetime.

Error source	Systematic error (ps)
momentum estimation	0.02
mass uncertainty	0.04
Λ_b purity	0.03
background b-content	0.02
fit range	0.02
selection cut	0.07
total systematic error	0.10

The systematic error has been computed from the spread of results obtained from various fits done by varying within their errors

– the Λ_b purity ($\pm 10\%$);
– the b-purity ($\pm 4\%$) of the background with decays in flight;
– the lower and upper limits of the time interval used in the fit by the error (± 0.45 ps) on the mean lifetime of the signal. The time interval determines the normalisation in the likelihood fit.

Finally it was checked that the fit result was stable within a 7% variation when changing the momentum cut for the track selection in the vertex algorithm in the range 0.3–1.2 GeV/c. This changes the probability of creating a fake vertex using tracks from the primary vertex; the above variation is considered as an upper limit on the systematic error on the lifetime from this source. The contributions of different sources of systematic errors, listed in table 2, were summed in quadrature, giving an overall systematic error of ± 0.10 ps.

The effect of the uncertainty of the background lifetime is included in the statistical error obtained from the fit, since the background and the signal lifetimes are determined at the same time. The final result for the Λ_b lifetime is then

$$\tau(\Lambda_b) = 1.04^{+0.48}_{-0.38} \pm 0.10 \text{ ps}.$$

8. Conclusions

An excess of 30 ± 10 Λl^- events compared with Λl^+ events is observed and is interpreted as a signal of semileptonic Λ_b decays. Assuming that most of the

weakly decaying b flavoured baryons produced in the Z^0 decay are Λ_b, the corresponding product branching ratio $f(b \to \Lambda_b) \times \mathrm{Br}(\Lambda_b \to \Lambda l\nu X)$ is determined to be $(0.41 \pm 0.13 \pm 0.09\%)$.

From a sub-sample of 18 decay vertices reconstructed in the muon data sample the Λ_b lifetime has been measured to be $\tau(\Lambda_b) = 1.04^{+0.48}_{-0.38} \pm 0.10$ ps.

Acknowledgement

References

[1] UA1 Collab., C. Albajar et al., Phys. Lett. B 273 (1992) 540.

[2] ALEPH Collab., D. Decamp et al., Phys. Lett. B 278 (1992) 209;
ALEPH Collab., D. Buskulic et al., Phys. Lett. B 297 (1992) 449.

[3] OPAL Collab., P.D. Acton et al., Phys. Lett. B 281 (1992) 394.

[4] W. Kwong and J. Rosner, Phys. Rev. D 44 (1991) 212.

[5] DELPHI Collab., P. Aarnio et al., Nucl. Instrum. Methods A 303 (1991) 233.

[6] DELPHI Collab., Preliminary results from 1991 data on the Z^0 resonance parameters and its electroweak couplings, DELPHI 92-29, PHYS 164, contributed to Rencontres de Moriond (March 1992).

[7] T. Sjöstrand et al., Comput. Phys. Commun. 39 (1986) 346; 43 (1987) 347.

[8] DELPHI Collab., P. Abreu et al., Phys. Lett. B 276 (1992) 536.

[9] DELPHI Collab., P. Abreu et al., Z. Phys. C 56 (1992) 47.

[10] P. Bambade and P. Zalewski, Electron identification in hadronic jets, DELPHI 92-32, PROG 183.

[11] DELPHI Collab., DELPHI event generation and detector simulation, DELPHI 87-97, PROG 100.

[12] Particle Data Group, K. Hikasa et al., Review of particle properties, Phys. Rev. D 45, part 2 (1992).

[13] ARGUS Collab., H. Albrecht et al., Phys. Lett. B 249 (1990) 359.

[14] CLEO Collab., G. Crawford et al., Phys. Rev. D 45 (1992) 752.

[15] DELPHI Collab., P. Abreu et al., Phys. Lett. B 281 (1992) 383.

[16] DELPHI Collab., A measurement of B-mesons production and lifetime using D-lepton events in Z^0 decays, CERN-PPE/92-174, submitted to Z. Phys. C.